Article

Synthesis of 5-Fluoropyrimidine Nucleotides as Sensitive NMR Probes of RNA Structure

Mirko Hennig, Lincoln G. Scott, Edit Sperling, Wolfgang Bermel, and James R. Williamson

J. Am. Chem. Soc., **2007**, 129 (48), 14911-14921 • DOI: 10.1021/ja073825i

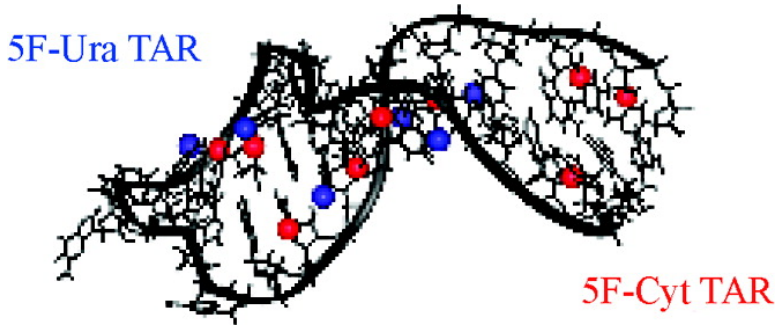

More About This Article

Additional resources and features associated with this article are available within the HTML version:

- Supporting Information
- Links to the 3 articles that cite this article, as of the time of this article download
- Access to high resolution figures
- Links to articles and content related to this article
- Copyright permission to reproduce figures and/or text from this article

View the Full Text HTML

J|A|C|S
ARTICLES
Published on Web 11/09/2007

Synthesis of 5-Fluoropyrimidine Nucleotides as Sensitive NMR Probes of RNA Structure

Mirko Hennig,*,§ Lincoln G. Scott,|| Edit Sperling,† Wolfgang Bermel,‡ and James R. Williamson*,†

Contribution from the Department of Molecular Biology and The Skaggs Institute of Chemical Biology, The Scripps Research Institute, MB 33, 10550 North Torrey Pines Road, La Jolla, California 92037, Bruker Biospin GmbH, Rheinstetten, Germany, Department of Biochemistry and Molecular Biology, Medical University of South Carolina, 173 Ashley Avenue, P.O. Box 250509, Charleston, South Carolina 29425, and Cassia, LLC, 4045 Sorrento Valley Boulevard, San Diego, California 92121

Received May 27, 2007; E-mail: jrwill@scripps.edu; hennig@musc.edu

Abstract: Enzymatic synthesis methods for the fluorinated 5′-triphosphate analogues 5F-UTP and 5F-CTP have been developed to facilitate ^{19}F-labeling of RNAs for biophysical studies. HIV-2 TAR RNAs were synthesized using these analogues by in vitro transcription reactions using T7 RNA polymerase. The uniform incorporation of 5F-U or 5F-C analogues into HIV-2 TAR RNA transcripts does not significantly alter the RNA structure or thermodynamic stability. Fluorine observed homonuclear ^{19}F−^{19}F and heteronuclear ^{19}F−^{1}H NOE experiments providing selective distance information are presented and discussed. The availability of efficient synthesis of 5F-UTP, and for the first time, 5F-CTP, will facilitate the use of 5F-labeled RNAs in structural, ligand binding, and dynamic studies of RNAs using the advantages of ^{19}F-labeling.

Introduction

Fluorine-19 (^{19}F) nuclear magnetic resonance (NMR) investigations of nucleic acids have been carried out for many years, due in large part to the favorable NMR properties of the ^{19}F nucleus.[1] Advantages of using spin ^{19}F as an NMR probe are its high sensitivity (83% of the ^{1}H) combined with 100% natural abundance and a wide chemical shift distribution (∼50-fold larger than that of ^{1}H). Fluorinated ribosomal 5S-rRNA[2] and tRNA[3] isolated from *E. coli* grown in the presence of 5-fluorouracil revealed high levels (>80%) of incorporation of 5-fluorouridine-5′-triphosphate (5F-UTP) in place of UTP. More recently, substantial effort has been made on the study of nucleic acids using both liquid- and solid-state ^{19}F NMR.[4−9] However, the limited availability of fluorinated nucleotides and limited data on the effects of their incorporation have restricted application of ^{19}F NMR to nucleic acids. Here, we report the efficient enzymatic synthesis and incorporation of 5F-UTP and 5-fluorocytidine-5′-triphosphate (5F-CTP) into RNA for NMR studies. Both 5F-UTP and 5F-CTP analogues are readily incorporated by T7 RNA polymerase into RNA transcripts in place of UTP and CTP, respectively. Furthermore, 5F-Ura- and 5F-Cyt-substituted RNAs, derived from the human immunodeficiency virus (HIV)-2 transactivation response element (TAR), are structurally and thermodynamically very similar to the wild-type TAR RNA, as demonstrated by comparative residual dipolar coupling (RDC) and thermal melting studies. The 5F-pyrimidine substitutions appear to be largely nonperturbing and are thus useful probes of RNA structure and dynamics using ^{19}F NMR.

Experimental Section

General. All materials used in the synthesis of 5-fluorouridine-5′-triphosphate and 5-fluorocytidine-5′-triphosphate were purchased from Sigma-Aldrich (St. Louis, MO), unless otherwise stated, and were used as received.

Cloning of Uridine Kinase (*udk*, EC 2.7.1.48). The gene encoding uridine kinase (EC 2.7.1.48) was cloned from the genome of *E. coli* strain MRE600 based on the reported gene sequence[10] using the sense primer 5′ GCG TCG GAA TTC ATG ACT GAT CAG TCT CAT CAG and anti-sense primer 3′ GGG CCC AAG CTT TCA TTA TTC AAA GAA CTG AC by standard PCR procedures. The *udk* gene product was ligated as a C-terminal fusion of maltose-binding protein

† The Scripps Research Institute.
‡ Bruker Biospin GmbH.
§ Medical University of South Carolina.
|| Cassia, LLC.

(1) Rastinejad, F.; Evilia, C.; Lu, P. *Methods Enzymol.* **1995**, *261*, 560−575.
(2) Marshall, A. G.; Smith, J. L. *J. Am. Chem. Soc.* **1977**, *99*, 635−636.
(3) Horowitz, J.; Ofengand, J.; Daniel, W. E., Jr.; Cohn, M. *J. Biol. Chem.* **1977**, *252*, 4418−4420.
(4) Hennig, M.; Munzarova, M. L.; Bermel, W.; Scott, L. G.; Sklenar, V.; Williamson, J. R. *J. Am. Chem. Soc.* **2006**, *128*, 5851−5858.
(5) Kreutz, C.; Kahlig, H.; Konrat, R.; Micura, R. *J. Am. Chem. Soc.* **2005**, *127*, 11558−11559.
(6) Kreutz, C.; Kahlig, H.; Konrat, R.; Micura, R. *Angew. Chem., Int. Ed.* **2006**, *45*, 3450−3453.
(7) Louie, E. A.; Chirakul, P.; Raghunathan, V.; Sigurdsson, S. T.; Drobny, G. P. *J. Magn. Reson.* **2006**, *178*, 11−24.
(8) Olsen, G. L.; Edwards, T. E.; Deka, P.; Varani, G.; Sigurdsson, S. T.; Drobny, G. P. *Nucleic Acids Res.* **2005**, *33*, 3447−3454.
(9) Torres, F. E.; Kuhnt, P.; De Bruyker, D.; Bell, A. G.; Wolkin, M. V.; Peeters, E.; Williamson, J. R.; Anderson, G. B.; Schmitz, G. P.; Recht, M. I.; Schweizer, S.; Scott, L. G.; Ho, J. H.; Elrod, S. A.; Schultz, P. G.; Lerner, R. A.; Bruce, R. H. *Proc. Natl. Acad. Sci. U.S.A.* **2004**, *101*, 9517−9522.
(10) Valentin-Hansen, P. *Methods Enzymol.* **1978**, *51*, 308−314.

(MBP) into the pMAL digested with *Eco*R1 and *Hin*dIII using phage T4 DNA ligase (New England Biolabs), incubating for 2 h at 25 °C. The ligation reaction mixture containing the resulting expression plasmid pUDK1 was used to transform *E. coli* JM109 cells by standard procedures.[11]

Preparation of Enzymes Used in the Synthesis of 5-Fluoro-Substituted NTPs. Ribokinase (*rbs*K, EC 2.7.1.15),[12] 5-phospho-D-ribosyl-α-1-pyrophosphate synthetase (*prs*A, EC 2.7.6.1),[12] and uracil phosphoribosyltransferase (*ura*P, EC 2.4.2.9)[13] were all purified from overexpressing strains as described previously. Uridine kinase was prepared from inducible strain JM109/pUDK1 grown in Luria−Bertani broth (per liter: 10 g of Tryptone, 5 g of yeast extract, 10 g of NaCl, 200 μg/mL ampicillin, Fisher Scientific) until mid log phase (A_{600} of 0.8) at 37 °C. The cells were induced for 4 h with the addition of 1 mM isopropyl-β-D-thiogalactopyranoside (IPTG) at 37 °C. After 4 h the cells were harvested by centrifugation at 6000*g* for 15 min (6000 rpm for a Sorval SLA-300 rotor). The cell pellet was resuspended in 20 mL of lysis buffer (50 mM potassium phosphate (pH 7.8), 5 mM 2-mercaptoethanol), and the cells were subjected to sonic disruption lysis. Cell debris was removed by centrifugation at 20 000*g* for 30 min (13 000 rpm for a Sorval SS-34 rotor). The clarified *udk* lysate was loaded to an amylose column preequilibrated with lysis buffer, and the partial purified MBP-*udk* was eluted with elution buffer (50 mM potassium phosphate (pH 7.8), 5 mM 2-mercaptoethanol, 10 mM maltose). Fractions containing the MBP-*udk* fusion were combined, an equal volume of glycerol was added, and the enzyme was stored at −20 °C.

Uridine Kinase Assay. Uridine kinase (*udk*, EC 2.7.1.48) activity was determined by spectrophotometric assay coupling consumption of ATP to NADH oxidation in a manner similar to that of the assay described previously for adenine phosphoribosyltransferase.[13] To the equilibrated assay solution (50 mM potassium phosphate, pH 7.5, 20 mM dithiothreitol, 10 mM $MgCl_2$, 5 mM ampicillin, 5.0 mM phosphoenolpyruvate, 0.5 mM ATP, 0.2 mM NADH, 0.1 mM kanamycin, 2 units of lactate dehydrogenase, 2 units of pyruvate kinase), *udk* was added to begin the assay. The change of absorbance at 340 nm that occurs when NADH is oxidized to NAD^+ was monitored as a function of time, with the activity being determined using a $\Delta\epsilon_{340}$ of 6220 cm^{-1} mol^{-1} for NADH.

Synthesis of 5-Fluorouridine-5′-triphosphate. In a round-bottom flask, D-ribose (150.1 mg, 1 mmol) and 5-fluorouracil (130.1 mg, 1 mmol) were dissolved in 200 mL of synthesis buffer (0.1 mM kanamycin, 0.5 mM ATP, 5 mM ampicillin, 10 mM $MgCl_2$, 20 mM dithiothreitol, 50 mM sodium 3-phosphoglycerate, 50 mM potassium phosphate, pH 7.5) at 37 °C. The synthesis was initiated by the addition of 50 units of ribokinase (*rbs*K, EC 2.7.1.15), 2 units of 5-phospho-D-ribosyl-α-1-pyrophosphate synthetase (*prs*A, EC 2.7.6.1), 2 units of uracil phosphoribosyltransferase (*ura*P, EC 2.4.2.9), 2 units of nucleoside monophosphate kinase (*pyr*H, EC 2.7.4.4), 75 units of adenylate kinase (*pls*A, EC 2.7.4.3), 150 units of pyruvate kinase (*pyr*F, EC 2.7.1.40), 300 units of 3-phosphoglycerate mutase (*yip*O, EC 5.4.2.1), and 100 units of enolase (*eno*, EC 4.2.1.11). The reaction was monitored by HPLC methods described elsewhere.[13] After 110 h, the synthesis of 5-fluorouridine-5′-triphosphate appeared to be complete. The solvent was removed in vacuo, the reaction was redissolved in 35 mL of 1 M triethylamine bicarbonate (pH 9.5), and proteins/salts were precipitated over 12 h at 4 °C. The insoluble material was removed by centrifugation at 20 000*g* (14 000 rpm for a Sorval SS-34 rotor), decanted, and solvent was removed in vacuo. The 5-fluorouridine-5′-triphosphate (0.8 mmol, 80% isolated yield) was dissolved in 10 mL of H_2O, the pH was adjusted to 7.6 with the addition of 1 M HCl, and it was used in transcription reactions without further purification. Data: ^{1}H NMR (600 MHz, D_2O) δ (mult.) 8.11 (d, $^3J_{HF}$ = 7.8 Hz, H-6), 5.98 (dd, $^5J_{HF}$ = 1.5 Hz, H-1′), 4.41 (dd, H-3′), 4.37 (dd, H-2′), 4.29 (dt, H-4′), 4.26 (dt, H-5′); ^{13}C NMR (150 MHz, D_2O) δ (mult) 162.0 (s, C-4), 152.9 (s, C-2), 143.4 (d, C-5), 128.0 (d, C-6), 91.1 (d, C-1′), 86.1 (d, C-4′), 76.4 (d, C-2′), 72.2 (d, C-3′), 67.7 (t, C-5′); ^{19}F NMR (564 MHz, D_2O) δ (mult.) −86.15 (dd, F-5).

Synthesis of 5-Fluorocytidine-5′-triphosphate. In a round-bottom flask, 5-fluorocytidine (100 mg, 0.38 mmol, ICN Biomedicals) was dissolved in 75 mL of the same synthesis buffer described above for the synthesis of 5F-UTP. The synthesis was started with the addition of 50 units of uridine kinase (*udk*, EC 2.7.1.48), 1 unit of nucleoside monophosphate kinase (*pyr*H, EC 2.7.4.4), 75 units of pyruvate kinase (*pyr*F, EC 2.7.1.40), 150 units of 3-phosphoglycerate mutase (*yip*O, EC 5.4.2.1), and 50 units of enolase (*eno*, EC 4.2.1.11). The reaction was monitored by HPLC methods described elsewhere.[13] After 72 h, the synthesis of 5-fluorocytidine-5′-triphosphate appeared to be complete. The 5-fluorocytidine-5′-triphosphate reaction was worked up in the same manner as that described above for 5F-UTP. The 5-fluorocytidine-5′-triphosphate (0.3 mmol, 78% isolated yield) was dissolved in 6 mL of H_2O, the pH was adjusted to 7.6 with the addition of 1 M HCl, and it was used in transcription reactions without further purification. Data: ^{1}H NMR (600 MHz, D_2O) δ (mult.) 8.22 (d, $^3J_{HF}$ = 6.3 Hz, H-6), 5.95 (dd, $^5J_{HF}$ = 1.5 Hz, H-1′), 4.40 (dd, H-3′), 4.34 (dd, H-2′), 4.31 (dd, H-5′), 4.30 (ddd, H-4′), 4.28 (dd, H-5″); ^{13}C NMR (150 MHz, D_2O) δ (mult) 159.0 (s, C-4), 155.3 (s, C-2), 139.4 (d, C-5), 129.2 (d, C-6), 92.2 (d, C-1′), 85.7 (d, C-4′), 77.0 (d, C-2′), 71.7 (d, C-3′), 67.2 (t, C-5′); ^{19}F NMR (564 MHz, D_2O) δ (mult.) −86.93 (dd, F-5).

In Vitro Transcription of RNA. Transcription reactions were carried out under the following conditions: 40 mM Tris-HCl (pH 8.1), 1 mM spermidine, 10 mM dithiothreitol, 0.01% Triton X-100, 80 mg/mL polyethyene glycol, 17 mM $MgCl_2$, 2 mM each nucleotide triphosphate, 0.3 μM template DNA (Operon), 0.3 μM promoter DNA (Operon), 2 unit/mL inorganic pyrophosphatase, 80 units/mL RNAse inhibitor (Promega), and 3000 units/mL T7 RNA polymerase.[14−16] The reactions were incubated for 4 h in a water bath at 37 °C, quenched with 0.1 volume of 0.5 M EDTA (pH 8.0), and extracted with an equal volume of phenol/chloroform (Fisher Scientific) equilibrated with TE buffer (10 mM Tris-HCl, 1 mM EDTA, pH 8.0). The aqueous layer was ethanol precipitated with the addition of 0.1 volume of 3 M sodium acetate, 3 volumes 100% ethanol at −20 °C. The crude RNA precipitate was first washed with 70% ethanol to remove extra salt, resuspended in 80% formamide stop buffer,[17] and purified on a 20% (29:1) acrylamide/bisacrylamide denaturing electrophoresis gel in TBE buffer (90 mM tris-borate, 2 mM EDTA, pH 8.1). The product band was identified by UV shadowing, excised, and elutrapped at 4 °C into TBE buffer for 4−6 h at 200 V with fractions taken each 1.5 h. The RNA was again ethanol precipitated. The purified RNA samples were concentrated and desalted using Centricon concentrators with 3 kDa molecular weight cutoff (Millipore). Two single 40 mL transcription reactions using single-stranded DNA templates yielded 1.73 and 0.88 μmol of 5F-Ura- and 5F-Cyt-substituted HIV-2 TAR RNA, respectively. The RNA samples were dissolved in the final NMR buffer.

NMR Spectroscopy. All ^{19}F NMR spectra were recorded on either 400 or 600 MHz Bruker Avance spectrometers equipped with 5 mm quadruple-resonance (^{1}H,^{13}C−^{19}F,^{31}P -QXI) probes with shielded triple axis gradients or on a Varian Inova 600 MHz spectrometer equipped with an actively shielded z-gradient triple-resonance (^{1}H−^{13}C,^{31}P) probe

(11) Hanahan, D. *J. Mol. Biol.* **1983**, *166*, 557−580.
(12) Tolbert, T. J.; Williamson, J. R. *J. Am. Chem. Soc.* **1996**, *118*, 7929−7940.
(13) Scott, L. G.; Tolbert, T. J.; Williamson, J. R. *Methods Enzymol.* **2000**, *317*, 18−38.
(14) Milligan, J. F.; Groebe, D. R.; Witherell, G. W.; Uhlenbeck, O. C. *Nucleic Acids Res.* **1987**, *15*, 8783−8798.
(15) Milligan, J. F.; Uhlenbeck, O. C. *Methods Enzymol.* **1989**, *180*, 51−62.
(16) Wyatt, J. R.; Chastain, M.; Puglisi, J. D. *BioTechniques* **1991**, *11*, 764−769.
(17) Sambrook, J.; Fritsch, E. F.; Maniatis, T.; Irwin, N.; Maniatis, T. *Molecular Cloning: a laboratory manual*, 2nd ed.; Cold Spring Harbor Laboratory Press: Cold Spring Harbor, NY, 1989.

with the inner coil detuned for ^{19}F detection. ^{1}H,^{1}H-NOESY spectra were recorded on an 800 MHz Bruker DRX spectrometer equipped with 5 mm triple-resonance (^{1}H−^{13}C,^{15}N -TXI) probe with shielded triple axis gradients. Carrier positions in the present work were −88.15 ppm for ^{19}F, and 7.12 (^{19}F,^{1}H-HOESY) or 4.79 (^{1}H,^{1}H-NOESY) ppm for ^{1}H, respectively. ^{1}H chemical shifts were externally referenced to DSS, with ^{19}F chemical shifts referenced indirectly according to the ^{19}F/^{1}H (TFA in a sphere)[18] ratio in DSS. All NMR experiments were recorded in NMR buffer (10 mM sodium phosphate buffer (pH 6.5), 150 mM NaCl) at 298 K unless otherwise stated. Four different HIV-2 TAR NMR samples were prepared with final sample concentrations ranging from ∼1.0 to 1.4 mM in 500 μL of H_2O/D_2O (9:1). Two uniformly 5F-Ura- and 5F-Cyt-labeled RNA samples were partially aligned by the addition of ∼25 mg/mL Pf1 phage (ASLA biotech Ltd., Riga, Latvia). Two uniformly 5F-Ura- and 5F-Cyt-labeled RNA HIV-2 ΔTAR NMR samples were prepared with final sample concentrations of ∼0.4 and 0.3 mM in 500 μL of H_2O/D_2O (9:1). All spectra were processed and analyzed using NMRPipe[19] and FELIX 2000 (MSI, San Diego, CA) program packages. Peak positions were determined using polynomial interpolation with Felix2000.

One-dimensional ^{19}F spectra were obtained by collecting 2048 complex points over a 5 kHz sweep width. Typically, 512 scans were accumulated with a recycle delay of 2.0 s. The data were multiplied by exponential functions corresponding to a line broadening of 4 Hz and zero-filled prior to Fourier transformation.

For the Water-flipback, Watergate ^{1}H,^{1}H-NOESY spectrum (recorded on 5F-Cyt-substituted TAR, τ_{mix} = 120 ms), 384 complex points were recorded with an acquisition time of 22.3 ms for ^{1}H (ω_1), and 2048 complex points with an acquisition time of 118.8 ms for ^{1}H (ω_2). A repetition delay of 1.4 s was used between transients, with 128 scans per increment (total measuring time 45.0 h). A solvent suppression filter was used in the ω_2 dimension to eliminate distortions from residual water prior to applying a Lorentz-to-Gauss window function. The ω_2 data were zero-filled before Fourier transformation. The ω_1 data were apodized with a 72° shifted squared sinebell window function and extensively zero-filled prior to Fourier transformation. The absorptive part of the final 2D matrix was 4096 × 2048 points.

For each ^{19}F,^{1}H-HOESY spectrum (τ_{mix} = 300 ms), 128 complex points were recorded with an acquisition time of 31.2 ms for ^{1}H (ω_1), and 1024 complex points with an acquisition time of 340.8 ms for ^{19}F (ω_2). A repetition delay of 1.2 s was used between transients, with 128 scans per increment (total measuring time 17.0 h). The ω_2 dimension was apodized using a Lorentz-to-Gauss window function. The ω_2 data were zero-filled before Fourier transformation. The ω_1 data were apodized with a squared cosinebell window function and zero-filled prior to Fourier transformation. The absorptive part of the final 2D matrix was 2048 × 256 points.

For the ^{19}F,^{19}F-NOESY spectrum (τ_{mix} = 400 ms), 64 complex points were recorded with an acquisition time of 31.9 ms for ^{19}F (ω_1), and 512 complex points with an acquisition time of 255.5 ms for ^{19}F (ω_2). A repetition delay of 1.8 s was used between transients, with 512 scans per increment (total measuring time 45.0 h). The ω_2 dimension was apodized using a Lorentz-to-Gauss window function. The ω_2 data were zero-filled before Fourier transformation. The ω_1 data were apodized with a squared cosinebell window function and zero-filled twice prior to Fourier transformation. The absorptive part of the final 2D matrix was 1024 × 256 points.

We adapted the spin-state selective (S^3)CT[20] experiment originally published by Lerche et al.[21] for measuring one-bond ^{1}H−^{15}N coupling constants to obtain residual dipolar one-bond ^{1}H−^{13}C coupling constants at natural ^{13}C abundance. A S^3CT duration of 1/(2J) = 2.9 ms optimized for aromatic ^{1}H,^{13}C correlations was chosen. For each ^{1}H,^{13}C-S^3CT subspectrum, 64 complex points were recorded with an acquisition time of 20.7 ms for ^{13}C (ω_1), and 1024 complex points with an acquisition time of 196.7 ms for ^{1}H (ω_2). A repetition delay of 1.2 s was used between transients, with 512 scans per increment (total measuring time 25.5 h). A solvent suppression filter was used in the ω_2 dimension to eliminate distortions from residual water prior to applying a Lorentz-to-Gauss window function. The ω_2 data were zero-filled twice before Fourier transformation. The ω_1 data were apodized with a 72° shifted squared sinebell window function and extensively zero-filled prior to Fourier transformation. The absorptive part of the final 2D matrices was 4096 × 256 points for each of the two ^{1}H,^{13}C-S^3CT subspectra, respectively.

Scheme 1

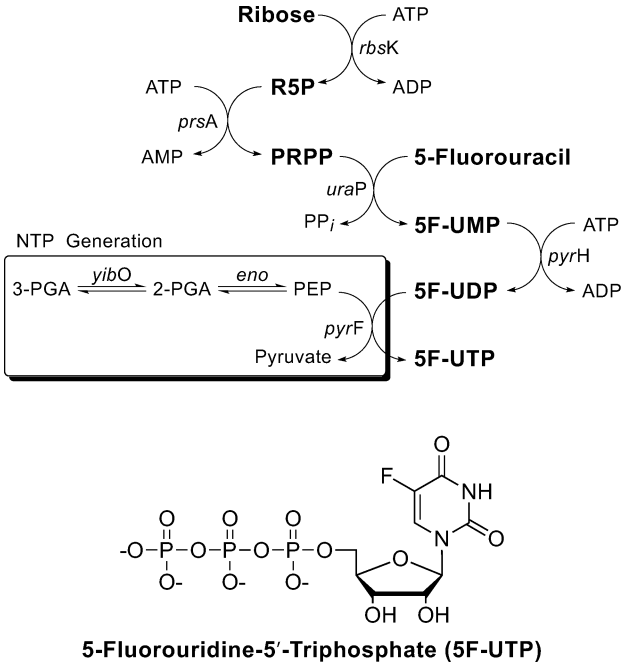

5-Fluorouridine-5′-Triphosphate (5F-UTP)

Thermal Melting Profiles. RNA thermal melting profiles were carried out on a temperature-controlled Cary-1 spectrophotometer (Varian) operated in single beam format. All thermal melting profiles were recorded in NMR buffer with the absorbance recorded as a function of temperature at 260 nm. Samples were prepared by first preannealing the RNA (1 μM) by heating at 95 °C for 2 min, then snap-cooling at 4 °C for 5 min. The annealed RNA was then added to a room-temperature cuvette, and the cell was allowed to equilibrate at 25 °C for 30 min. The temperature controller was ramped at a rate of 1 °C/min from 25 to 95 °C. Data points were collected every minute, and the temperature was accurately determined by a temperature probe inserted into a cuvette containing NMR buffer. Melting temperature (T_m) and the enthalpy of unfolding at the melting temperature ($\Delta H_m°$) were calculated by nonlinear least-squares fits to the van't Hoff equation, using Igor software (Wavemetrics).[22] The change in the heat capacity (ΔC_p) upon unfolding was assumed to be zero.

Results

Preparation of 5-Fluorouridine-5′-triphosphate. The preparation of 5-fluorouridine-5′-triphosphate (5F-UTP) was carried out using an adaptation of an enzymatic synthesis method developed previously (Scheme 1).[12] The base analogue 5-fluorouracil is readily used as a substrate for uracil phosphoribosyl transferase (*uraP*), which provides a novel and efficient route

(18) Maurer, T.; Kalbitzer, H. R. *J. Magn. Reson., Ser. B* **1996**, *113*, 177−178.
(19) Delaglio, F.; Grzesiek, S.; Vuister, G. W.; Zhu, G.; Pfeifer, J.; Bax, A. *J. Biomol. NMR* **1995**, *6*, 277−293.
(20) Sorensen, M. D.; Meissner, A.; Sorensen, O. W. *J. Biomol. NMR* **1997**, *10*, 181−186.
(21) Lerche, M. H.; Meissner, A.; Poulsen, F. M.; Sorensen, O. W. *J. Magn. Reson.* **1999**, *140*, 259−263.
(22) Puglisi, J. D.; Tinoco, I., Jr. *Methods Enzymol.* **1989**, *180*, 304−325.

Scheme 2

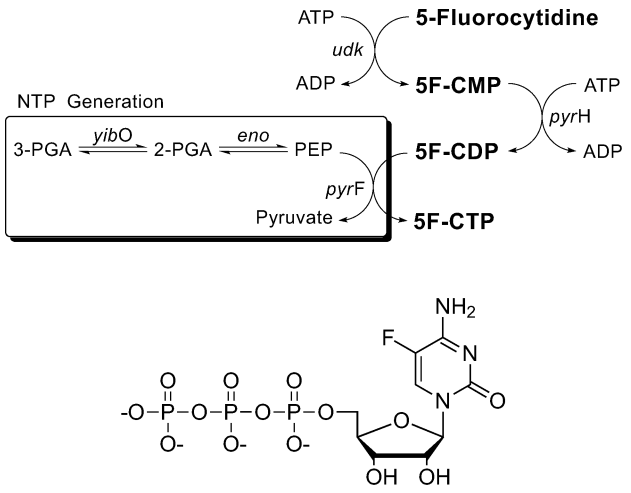

5-Fluorocytidine-5′-Triphosphate (5F-CTP)

to produce 5F-UMP, and ultimately 5F-UTP, as shown in Scheme 1. This method is also readily adaptable to include selective deuteration, using enzymes of the glycolysis, pentose phosphate, nucleotide biosynthesis, and salvaging pathways.[13,23]

The conversion of ribose into 5F-UTP begins with the phosphorylation of ribose, first at the C-5 hydroxyl group catalyzed by ribokinase (*rbs*K), then at the C-1 position by 5-phospho-D-ribosyl-α-1-pyrophosphate synthetase (*prs*A) forming PRPP. The coupling of 5-fluorouracil to PRPP is catalyzed by uracil phosphoribosyltransferase (*ura*P), forming 5-fluorouridine-5′-monophosphate (5F-UMP). Nucleoside monophosphates are converted to the corresponding triphosphates using pyrimidine specific nucleoside monophosphate kinase (*pyr*H), adenylate kinase (*pls*A), and pyruvate kinase (*pyr*F). This synthesis of 5F-UTP requires 5 equiv of ATP, which is supplied by phosphoenolpyruvate (PEP) and is made in situ from excess sodium 3-phosphoglycerate (3-PGA) through the coupled action of 3-phosphoglycerate mutase (*yip*O) and enolase (*eno*).[24,25]

Preparation of 5-Fluorocytidine-5′-triphosphate. Unfortunately, the route analogous to Scheme 1 cannot be used for preparation of 5F-CTP. There is no known ribosyl transferase activity for coupling cytosine to PRPP, and cellular CTP is synthesized directly from UTP by CTP synthase (*pyr*G). However, because 5F-UTP is not a substrate for *pyr*G,[26] an alternate route beginning with the 5F-cytidine nucleoside must be used (Scheme 2).

The synthesis begins with the phosphorylation of the nucleoside analogue 5-fluorocytidine at the C-5′ hydroxyl group catalyzed by uridine kinase (*udk*), forming 5F-CMP.[10] In analogy to the method used to prepare 5F-UTP, the pyrimidine nucleoside monophosphate 5F-CMP is converted to the corresponding triphosphate using nucleoside monophosphate kinase (*pyr*H) and pyruvate kinase (*pyr*F). This synthesis of 5F-CTP requires 3 equiv of ATP, which is supplied by phosphoenolpyruvate (PEP) as described above.[24,25]

Incorporation of 5F-Pyrimidines into HIV-2 TAR RNA. The HIV-2 TAR RNA is comprised of two A-form helical stem segments that are separated by a two-nucleotide bulge (U23 and U25), and the upper stem is capped by an apical hexanucleotide loop (C30-A35). To assess the effects of 5F-pyrimidine substitution on RNA structure and stability, HIV-2 TAR RNAs were synthesized by in vitro transcription containing either 5F-UTP or 5F-CTP, as 5F-Ura-TAR and 5F-Cyt-TAR, respectively. The 5F-UTP and 5F-CTP were efficiently incorporated into the full-length RNA transcript, and the overall yields were comparable to those with unlabeled nucleotides. Two related control molecules, where the characteristic bulge of TAR is deleted, were also prepared as 5F-Ura-ΔTAR and 5F-Cyt-ΔTAR.

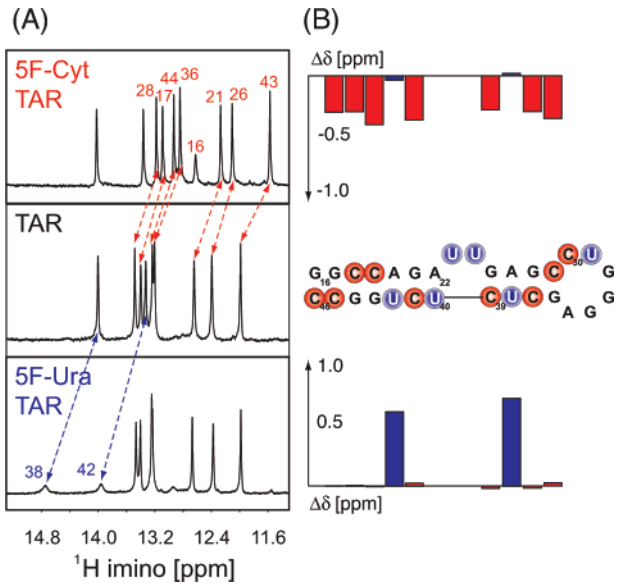

Figure 1. (A) One-dimensional jump-return echo NMR spectra[30] showing the imino region of 5F-Cyt-substituted TAR (top), unmodified TAR (middle), and 5F-Cyt-substituted TAR (bottom) recorded under identical conditions (10 mM sodium phosphate buffer (pH 6.4), 50 mM NaCl, and 0.1 mM EDTA, 298 K) at 800 MHz proton resonance frequency. Assignments for observable imino protons are indicated. (B) Sequence and secondary structural representation of HIV-2 TAR. 5-Fluorocytidine substitutions are highlighted by red and 5-fluorouridine substitutions are highlighted by blue circles, respectively. The chemical shift changes $\Delta\delta$ ($\Delta\delta$[ppm] = δ_{wt-TAR}[ppm] − $\delta_{5F-Ura/Cyt-TAR}$[ppm]) of observable imino resonances induced by the 5F-Ura/Cyt substitutions are symbolized in a bar plot. Individual changes are shown above the respective base-pair and assigned using residue numbers.

The imino proton spectra for 5F-Ura-TAR, 5F-Cyt-TAR, and unlabeled TAR are shown in Figure 1A. From the number of observable imino protons, all expected base-pairs appear to form, and additional resonances are observable in the labeled samples. The resonance assignments in the labeled samples were obtained from a water flip-back, WATERGATE ^{1}H,^{1}H-NOESY spectrum measured at 800 MHz (Supporting Information Figure 1).[27] All 5F-Ura and 5F-Cyt pyrimidine analogues in stem segments of TAR are hydrogen-bonded and engaged in Watson−Crick 5F-U−A or 5F-C−G base-pairs. Unpaired 5F-Ura and 5F-Cyt nucleotides are found in the loop and bulge structural elements (Figure 1B).

Shielding or deshielding effects attributable to the presence of a fluorine substituent can be studied by comparing chemical shifts of the protons in a fluorine-substituted RNA with the

(23) Tolbert, T. J.; Williamson, J. R. *J. Am. Chem. Soc.* **1997**, *119*, 12100−12108.
(24) Hirschbein, B. L.; Mazenod, F. P.; Whitesides, G. M. *J. Org. Chem.* **1982**, *47*, 3765−3766.
(25) Simon, E. S.; Grabowski, S.; Whitesides, G. M. *J. Org. Chem.* **1990**, *55*, 1834−1841.
(26) Scheit, K. H.; Linke, H. J. *Eur. J. Biochem.* **1982**, *126*, 57−60.
(27) Lippens, G.; Dhalluin, C.; Wieruszeski, J. M. *J. Biomol. NMR* **1995**, *5*, 327−331.

Table 1. Fluorine and Proton Chemical Shifts for 5F-Pyrimidine-Substituted TAR, and Differences in Chemical Shifts between Modified and Unmodified RNA

nucleotide	$\delta(^{19}F5)$ [ppm][a]	$\delta(^1H1)$ [ppm][b]	$\delta(^1H3)$ [ppm][b]	$\delta(^1H42/^1H41)$ [ppm][b]	$\Delta\delta_{5F-C}$ ($^1H1$) [ppm][c]	$\Delta\delta_{5F-U}$ ($^1H1$) [ppm][d]	$\Delta\delta_{5F-C}$ ($^1H3$) [ppm][c]	$\Delta\delta_{5F-U}$ ($^1H3$) [ppm][d]	$\Delta\delta_{5F-C}$ ($^1H42/^1H41$) [ppm][c]
G16		*12.625*[e]			n.d.[h]	n.d.[h]			
G17		13.400			−0.309	0.004			
C18	−88.34			8.566/6.822					0.453/0.618
C19	−89.19			8.314/6.808					0.513/0.535
G21		12.644			−0.374	0.026			
U23	−86.60		n.d.[f]				n.d.[h]	n.d.[h]	
U25	−86.62		n.d.[f]				n.d.[h]	n.d.[h]	
G26		12.393			−0.287	−0.020			
G28		13.482			−0.303	−0.017			
C29	−88.77			n.d.[f]/6.800					−/0.551
C30	−87.56			*8.581/7.422*[g]					n.d.[h]
U31	−86.56		n.d.[f]				n.d.[h]	n.d.[h]	
G36		13.204			−0.361	0.028			
C37	−89.52			8.604/6.795					0.439/0.507
U38	−89.54		14.003				0.021	0.743	
C39	−88.28			8.314/6.902					0.502/0.513
U40	−88.28		n.d.[f]				n.d.[h]	n.d.[h]	
C41	−87.95			8.254/6.985					0.468/0.483
U42	−89.39		13.327				−0.037	0.629	
G43		11.987			−0.414	−0.005			
G44		13.236			−0.304	0.007			
C45	−88.77			8.577/6.851					0.429/0.597
C46	−88.86			*8.826/7.483*[e]					n.d.[h]

[a] ^{19}F chemical shifts obtained at 308 K in H_2O/D_2O (95%/5%) were referenced indirectly according to $^{19}F/^1H$ (TFA in a sphere)[18] chemical shift ratios in DSS. [b] ^1H chemical shifts were externally referenced to DSS. [c] Chemical shift changes $\Delta\delta$ ($\Delta\delta$[ppm] = $\delta_{5F-Cyt-TAR}$[ppm] − δ_{wt-TAR}[ppm]) induced by the 5F-cytidine substitutions. [d] Chemical shift changes $\Delta\delta$ ($\Delta\delta$[ppm] = $\delta_{5F-Ura-TAR}$[ppm] − δ_{wt-TAR}[ppm]) induced by the 5F-uridine substitutions. [e] ^1H chemical shifts obtained from $^1H,^1H$-NOESY using 5F-cytidine-substituted TAR; broadened beyond detection in unmodified TAR. [f] Insufficiently resolved or too broad for accurate measurement. [g] ^1H chemical shifts obtained from $^{19}F,^1H$-HOESY using 5F-cytidine-substituted TAR; broadened beyond detection in unmodified TAR. [h] Not determined due to missing reference chemical shift δ_{wt-TAR}[ppm].

chemical shifts of the same protons in the unmodified, reference RNA. Recently, we reported on selected shielding or deshielding effects attributable to the presence of the 5-fluoropyrimidine substitutions incorporated into TAR.[4] As expected, the influence of fluorine substitutions on chemical shifts of base H6 protons is pronounced due to close proximity to the fluorine atom. All base H6 protons are deshielded ($\Delta\delta \approx 0.21$ ppm) as a consequence of the strongly electron-withdrawing nature of the fluorine substituent, whereas essentially no chemical shift effects are observed for the more distant anomeric H1′ protons. A comparative analysis of imino H3 of 5-fluorouridine as well as guanine imino H1 and amino H41/H42 protons of 5-fluorocytidine in modified TAR RNA derived from homonuclear $^1H,^1H$-NOESY reveals marked shift perturbations for all exchangeable protons observed (Figure 1B and Table 1). The 5-fluorouridine H3 imino protons of U42 and U38 are noticeably broadened as compared to the uridine imino protons in the wild-type TAR RNA as a consequence of the 5-fluorouridine N3 nitrogen pK_a, which is not too far from physiological pH (Figure 1A).[28,29]

The considerable electronegativity of fluorine influences the pK values of neighboring groups. The presence of a fluorine atom at the C5 position substantially lowers the apparent N3 nitrogen pK_a by 1.7−1.8 units, to 7.6 and 2.3 for 5-fluorouridine and 5-fluorocytidine, respectively.[31,32]

The observed 5-fluorouridine H3 imino proton line widths are approximately 70 and 80 Hz for 5F-U38 and 5F-U42 at 298 K and pH 6.5, respectively, while no appreciable broadening is observed for guanine imino protons (linewidth <20 Hz). Furthermore, the U42 and U38 imino protons in 5-fluorouridine-substituted TAR are deshielded and experience pronounced downfield chemical shift changes as compared to the unmodified RNA ($\Delta\delta = \delta_{5F-Ura-TAR} - \delta_{wt-TAR}$ of 0.63 and 0.74 ppm, respectively, Figure 1B) due to the presence of the ^{19}F-nuclei. At the same time, chemical shifts of guanine imino protons shown in Figure 1B involved in canonical G−C base-pairs remain virtually unchanged ($\Delta\delta_{average}$(G H1) = 0.003 ± 0.019 [ppm]). While the increased line width of the 5F-uridine imino protons presents practical limitations for measuring proton NOEs, we do readily observe NOEs to these protons at lower temperatures (see Supporting Information). However, the ^{19}F-nucleus provides compensating new observables described below.

In contrast, the exchangeable guanine imino protons in 5-fluorocytidine-substituted TAR are more shielded and shift upfield as compared to the unmodified RNA ($\Delta\delta_{average}$(G H1) = −0.336 ± 0.151 [ppm]) due to the presence of the ^{19}F-nuclei on the complementary base involved in the Watson−Crick 5F-C−G base-pair (Figure 1A). Interestingly, the exchangeable uridine U42 and U38 imino protons that are engaged in canonical U−A base-pairs do not experience chemical shift changes greater than ±0.04 ppm. Evidently, the 5-fluorocytidine substitutions do not disturb hydrogen-bonding interactions in Watson−Crick geometry, and 5F-C−G base-pairs featuring regular amino tautomeric configurations are formed. We observe

(28) Sahasrabudhe, P. V.; Gmeiner, W. H. *Biochemistry* **1997**, *36*, 5981−5991.
(29) Sahasrabudhe, P. V.; Pon, R. T.; Gmeiner, W. H. *Biochemistry* **1996**, *35*, 13597−13608.
(30) Sklenar, V.; Brooks, B. R.; Zon, G.; Bax, A. *FEBS Lett.* **1987**, *216*, 249−252.
(31) Alderfer, J. L.; Loomis, R. E.; Sharma, M.; Hazel, G. *Prog. Clin. Biol. Res.* **1985**, *172A*, 249−261.
(32) Wempen, I.; Fox, J. J.; Kaplan, L.; Duschinsky, R. *J. Am. Chem. Soc.* **1961**, *83*, 4755.

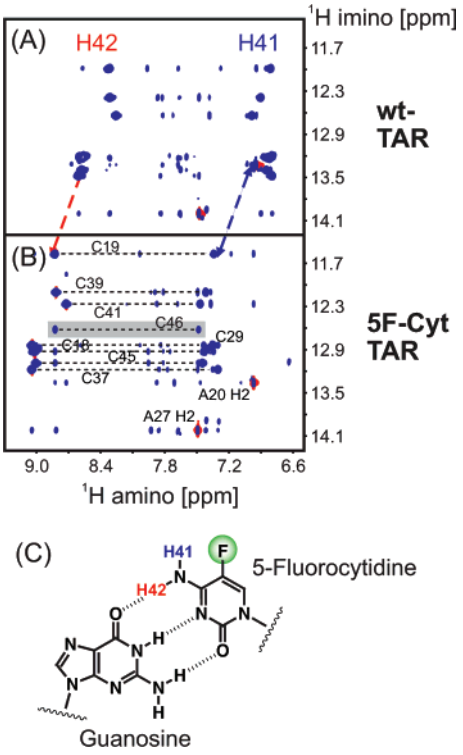

Figure 2. Water-flipback, Watergate ^{1}H,^{1}H-NOESY experiments[27] recorded on a four-channel Bruker DRX 800 MHz spectrometer at a temperature of 298 K showing (A) imino (ω_1) to amino (ω_2) hydrogen connectivities for unmodified TAR, and (B) corresponding connectivities for 5F-Cyt-substituted TAR. Negative contours are shown in red. The NOESY mixing times τ_{mix} were 120 ms. Assignments of individual 5-fluorocytidine homonuclear guanine imino to 5-fluorocytidine amino and uridine imino to adenine H2 NOESY cross-peaks are given. A gray box highlights the G16 imino (ω_1) to 5F-C46 amino (ω_2) hydrogen NOE correlations that are broadened beyond detectable limits in unmodified TAR. (C) Chemical structure of modified 5-fluorocytidine to guanine Watson−Crick-type base-pair.

substantial downfield shifts for both amino H41/H42 hydrogens induced by the presence of the ^{19}F-nuclei at the C5 position of cytosine in modified TAR RNA (Figure 2). This has been previously reported for a single 2′-deoxy-5-fluorocytidine incorporated into small DNA duplexes.[33] Interestingly, the upfield H41 amino proton, which is in closer proximity to the ^{19}F-nucleus, is more deshielded ($\Delta\delta_{average}$(5F-C H41) = 0.543 ± 0.049 [ppm]) as compared to the downfield H42 amino proton ($\Delta\delta_{average}$(5F-C H42) = 0.467 ± 0.034 [ppm]). Typically, fraying at the termini of helices enhances solvent exchange of imino and amino protons with bulk water. Exchangeable G H1 imino and C H41/42 amino proton intensities are greatly diminished at 298 K and pH 6.5. However, exchangeable base protons in the terminal Watson−Crick 5F-C46−G16 base-pair in 5-fluorocytidine-substituted TAR are detectable, indicating slowed exchange with bulk solvent.

Secondary Structure of 5-Fluoropyrimidine-Modified RNA Monitored by ^{19}F Chemical Shifts. The ^{19}F resonances were assigned for each 5-fluorouridine and 5-fluorocytidine in the substituted TAR RNA samples,[4] as shown in Figure 3. A 5-fold increase in chemical shift dispersion was observed comparing base F5 to H5 resonances, in line with the generally acknowledged pronounced sensitivity of fluorine shielding parameters to changes in the local environment. The observed chemical shift dispersion in the 5F-Ura- and 5F-Cyt-substituted HIV-2 TAR RNAs is 3.1 ppm (Table 1), reflecting the different microenvironments and stacking arrangements of each fluorinated base (Figure 3).

The ^{19}F chemical shifts serve as sensitive markers of RNA secondary structure, and significant shift differences are observed between Watson−Crick and unpaired nucleotides. For example, 5F-U25 and 5F-U23, located in the TAR bulge, are deshielded and shifted by approximately 3.0 ppm to lower fields as compared to 5F-U42 and 5F-U38 that adopt Watson−Crick geometries. Similarly, the loop nucleotide 5F-C30 is the most deshielded among all 5F-Cyt pyrimidine substitutions. The intermediate ^{19}F chemical shift of 5F-U40 is diagnostic for weakened stacking interactions caused by distortions and twist introduced by the opposing bulge. Consistent with the atypical U40-A22 Watson−Crick pairing geometry in the free TAR RNA structure, the corresponding U40 imino proton is severely exchange-broadened at 298 K and thus not observable in 90% H_2O, 10% D_2O.[34−36]

The effect of the bulge structure on nearby ^{19}F chemical shifts was determined from the spectra of the bulge-deleted ΔTAR RNA (Figure 3A). The chemical shift changes $\Delta\delta$ ($\Delta\delta$[ppm] = $\delta_{wt-5F-TAR}$[ppm] − $\delta_{5F-\Delta TAR}$[ppm]) induced by the deletion of bulged nucleotides U23 and U25 are substantial for flanking residues. Canonical stacking interactions in the bulge-deleted ΔTAR RNA give rise to strong shielding effects for U40 ($\Delta\delta$ = −1.7 ppm), C41 ($\Delta\delta$ = −0.7 ppm), and C39 ($\Delta\delta$ = −0.5 ppm) with respect to the reference wild-type TAR RNA (Figure 3B). The $\Delta\delta$ comparison also allowed for unambiguous assignments of U23, U25, U40, C41, and C39 by simple comparison of the original 5F-Ura- and 5F-Cyt-substituted TAR spectra with the deletion mutant spectra.

The responsiveness of ^{19}F chemical shifts to environmental factors is a result of shielding effects from several sources, but reports in the literature differ in the relative importance of individual contributions in proteins.[37,38] Base stacking appears to be a dominant shielding effect in RNA and can be qualitatively monitored by comparative chemical shift analysis. Fluorine nuclei are expected to be shielded by neighboring, stacked nucleobases in canonical A-form helical RNA. These stacking interactions are less pronounced in regions of irregular, non A-form secondary structure, which is accompanied by deshielding or shifts to lower fields.

Heteronuclear Through-Space ^{19}F,^{1}H-HOESY Experiments. The nuclear Overhauser effect (NOE) is an established tool for the structure elucidation of molecules in solution.[39] Homonuclear ^{1}H,^{1}H-NOESY measurements are routinely applied and extensively used to investigate biomolecular structures. Heteronuclear NOEs also provide distance information. The basic X,^{1}H-HOESY sequence was introduced by Rinaldi and Levy using X = ^{13}C.[40,41] The sensitivity of HOESY spectra

(33) Sowers, L. C. *J. Biomol. Struct. Dyn.* **2000**, *17*, 713−723.
(34) Aboul-ela, F.; Karn, J.; Varani, G. *Nucleic Acids Res.* **1996**, *24*, 3974−3981.
(35) Hennig, M.; Williamson, J. R. *Nucleic Acids Res.* **2000**, *28*, 1585−1593.
(36) Long, K. S.; Crothers, D. M. *Biochemistry* **1999**, *38*, 10059−10069.
(37) de Dios, A. C.; Pearson, J. G.; Oldfield, E. *Science* **1993**, *260*, 1491−1496.
(38) Gregory, D. H.; Gerig, J. T. *Biopolymers* **1991**, *31*, 845−858.
(39) Neuhaus, D.; Williamson, M. P. *The Nuclear Overhauser Effect in Structural and Conformational Analysis*; Wiley and Sons: New York, 1989; p 522.
(40) Rinaldi, P. L. *J. Am. Chem. Soc.* **1983**, *105*, 5167−5168.
(41) Yu, C.; Levy, G. C. *J. Am. Chem. Soc.* **1984**, *106*, 6533−6537.

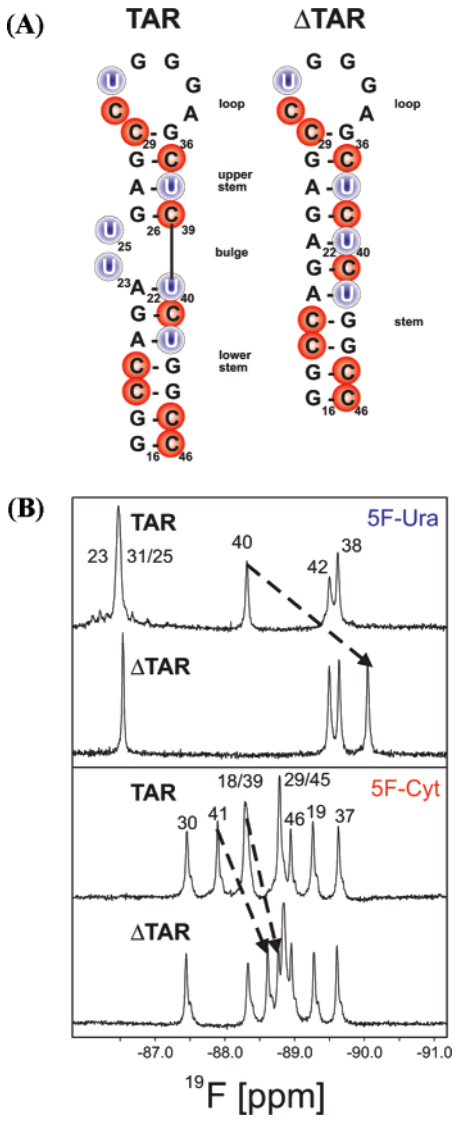

Figure 3. (A) Sequence and secondary structural representation of HIV-2 TAR and bulge deleted ΔTAR RNA with 5-fluorocytidine substitutions highlighted by red and 5-fluorouridine substitutions highlighted by blue circles, respectively. (B) One-dimensional ^{19}F spectra of 5-fluorocytidine- and 5-fluorouridine-substituted TAR and ΔTAR recorded without ^{1}H decoupling at 564.6 MHz (^{19}F resonance frequency) at 303 K. Assignments for ^{19}F resonances are indicated, and dashed lines connect the resonance frequencies of U40, C41, and C39 in the wild-type and deletion mutant RNA molecules.

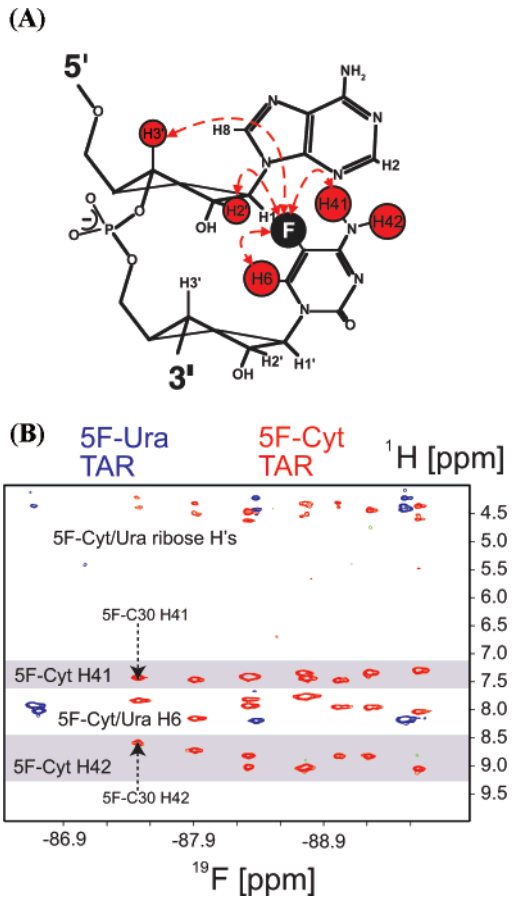

Figure 4. (A) Schematic representation of a 5′-ApC-3′ dinucleotide with arrows indicating the short, observable intra- and interresidual distances between the F5 nuclei and cytidine H41/42 amino, base H6, and ribose H2′/3′ protons. (B) Fluorine-detected ^{19}F,^{1}H-HOESY (^{19}F resonance frequency of 564.6 MHz) showing NOE cross-peaks between F5 nuclei and cytidine H41/42 amino, base H6, and ribose H2′/3′ protons (5F-Ura labeled TAR in blue, 5FCyt-labeled TAR in red). Arrows point to the 5F-C30 amino (ω_1) to 5F-C30 fluorine (ω_2) NOE correlations. These amino protons are broadened beyond detectable limits in unmodified TAR. The HOESY mixing times τ_{mix} were 300 ms. High power proton pulses were applied with a field strength of 26.3 kHz, while high power ^{19}F pulses were applied with a field strength of 11.6 kHz.

suffers from the inherent drawbacks of X nucleus detection, such as low resolution in the indirect (ω_1) ^{1}H dimension, low natural abundance, and low gyromagnetic ratios γ(X).

However, heteronuclear ^{19}F,^{1}H NOEs are readily accessible due to the high gyromagnetic ratio and the 100% natural abundance of ^{19}F. The ^{19}F,^{1}H NOE assumes a value of 0.5 in the extreme narrowing limit, passes through zero before finally approaching its maximum value of −1 for slowly tumbling macromolecules. Another distinct advantage of ^{19}F-detection is that solvent suppression is unneeded due to the lack of background ^{19}F in commonly used solvents, and ^{19}F,^{1}H-HOESY has been employed to investigate the conformational properties of chemically synthesized 5F-Ura-substituted 16-mer ssRNA (single-stranded RNA)[42] and of DNA duplex and hairpin structures carrying 2′-deoxy-5-fluorouridine substitutions.[43] Phase-sensitive ^{19}F,^{1}H-HOESY spectra for the 5-fluoropyrimidine substituted TAR RNA samples are shown in Figure 4. The ^{19}F,^{1}H dipole−dipole relaxation is dominated by the interaction between F5 and the base H6 proton for 5-fluoropyrimidines, for which the internuclear distance is 2.58 Å (Figure 4).[44] Neighboring amino protons in 5-fluorocytidine-substituted TAR RNA are nondegenerate because of the slow rotation of the exocyclic C4−N4 amino nitrogen bond. Consequently, each 5-fluorocytidine amino group provides two additional, strong heteronuclear ^{19}F,^{1}H NOEs to separate well-resolved H41 and H42 amino protons. The more distant, downfield shifted H42 amino proton typically participates in hydrogen-bonding interaction with the opposing guanine O6 oxygen. Nevertheless, heteronuclear ^{19}F,^{1}H cross-peaks involving both H41 and H42 amino protons are observed because the proximal, upfield shifted H41 mediates efficient spin diffusion and effectively relays magnetization between the geminal amino protons. Intense ^{19}F,^{1}H NOEs are observed from all of the amino protons

(42) Collier, A. K.; Arnold, J. R. P.; Fisher, J. *Magn. Reson. Chem.* **1996**, *34*, 191−196.

(43) Metzler, W. J.; Leighton, P.; Lu, P. *J. Magn. Reson.* **1988**, *76*, 534−539.
(44) Voet, D. H.; Rich, A. *J. Am. Chem. Soc.* **1969**, *91*, 3069−3075.

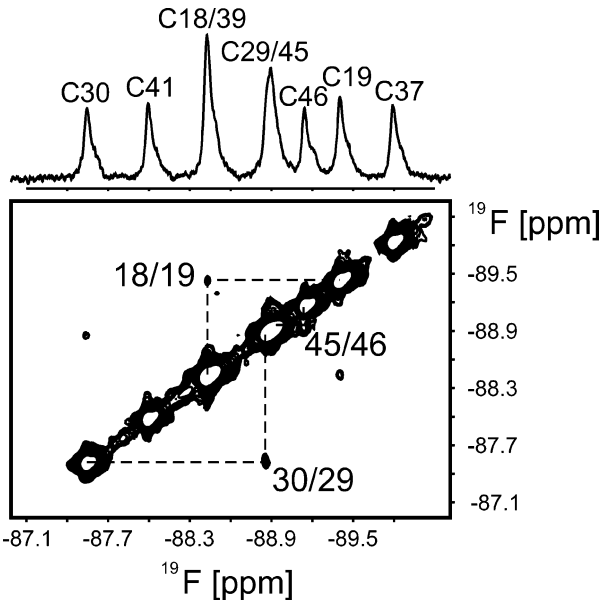

Figure 5. Phase-sensitive ^{19}F,^{19}F-NOESY experiments (^{19}F resonance frequency of 376.4 MHz) showing fluorine connectivities between stacked bases in 5F-Cyt-substituted TAR (bottom). Assignments of individual homonuclear ^{19}F-NOESY cross-peaks are given. The NOESY mixing time τ_{mix} was 400 ms. High power ^{19}F pulses were applied with a field strength of 25.0 kHz.

involved in the eight 5F-C−G Watson−Crick-type base-pairs. We were surprised to detect the unpaired, solvent-exposed amino protons of 5F-C30 located in the hexanucleotide TAR loop. In analogy to the fraying of terminal base-pairs, these exchangeable amino protons are usually broadened beyond detection in unmodified RNAs because of intermediate rotation around the exocyclic C4−N4 bond in combination with solvent exchange phenomena. The resonance separation between the downfield 5F-C30 H42 and the upfield H41 amino protons ($\delta_{H42-H41}$ = 1.159 ppm) at 298 K is smaller as compared to the average amino chemical shift difference ($\langle\delta_{H42-H41}\rangle$ = 1.508 ± 0.169 ppm) but still strongly suggests more hindered C4−N4 bond rotation for 5F-C even in the absence of base-pairing. The intensity of the 5F-C30 H42-F5 NOE correlation is noticeably reduced with respect to the related H41-F5 cross-peak.

Homonuclear Through-Space ^{19}F,^{19}F-NOESY Experiments. We employed a transient ^{19}F,^{19}F-NOE experiment that can easily be performed by adaptation of sequences designed for proton correlations, except that longer NOESY mixing times should be chosen ($\tau_{mix} \approx$ 400 ms) such that cross-peaks reach their maximum intensities. HIV-2 TAR contains three 5′-CpC-3′ and one 5′-UpU-3′ sequential pyrimidine−pyrimidine dinucleotides. Consecutive pyrimidines in segments adopting canonical A-form structure stack at ∼3.5 Å intervals, thus leading to relatively short distances between sequential ^{19}F5 nuclei. The only consecutive pair of uridine residues is located in the TAR bulge, which exhibits increased flexibility as compared to the more rigid, flanking A-form helices in the absence of ligands. We did not attempt to obtain direct evidence for the stacking of 5F-U25 to 5F-U23. However, a ^{19}F,^{19}F-NOESY experiment recorded at 400 MHz reveals all three consecutive 5-fluorocytidine dinucleotide connectivities (Figure 5). NOESY cross-peaks connecting 5F-C18/5F-C19, 5F-C29/5F-C30, and 5F-C45/5F-C46 are observable employing mixing times greater or equal to $\tau_{mix} \approx$ 400 ms. The most structured regions of the TAR apical loop are at either end of the loop, consistent with stacking of loop residues on the stem-closing base-pair. The detection of the 5F-C29/5F-C30 cross-peak confirms earlier studies reporting that the orientation of C30 allows efficient stacking on top of C29.[45,46]

Probing Global Structure of 5-Fluoropyrimidine-Substituted HIV-2 TAR RNAs Using RDCs. New experiments to measure orientational, rather than distance-dependent, dipolar couplings have been developed.[47,48] To determine if global RNA structure changes were caused by the 5-fluoropyrimidine substitutions, residual dipolar couplings (RDCs) were measured in partially aligned medium for the wild-type as well as 5-fluorouridine- and 5-fluorocytidine-substituted HIV-2 TAR RNAs. Partial alignment ensures that dipolar couplings no longer average to zero, while retaining the quality of high-resolution NMR spectra. We partially aligned 5-fluoropyrimidine-substituted TAR RNA using Pf1 bacteriophage solution.[49,50] We employed a ^{1}H,^{13}C-S^{3}CT element that allows for ^{1}J(H,C) coupling evolution, and subsequent phase cycling selects α or β spin states of aromatic carbons.[20] Two experiments are recorded in an interleaved manner, and postacquisition addition and subtraction creates the edited subspectra with the coupled aromatic proton spin in the ω_2 dimension[21] at natural ^{13}C abundance. The subspectra allow for the convenient measurement of ^{1}J(H,C) in isotropic phases and ^{1}J(H,C) + ^{1}D(H,C) in anisotropic phases, respectively. The pairwise rmsd for ^{1}J(C,H) coupling measurements for 5F-Ura- and 5F-Cyt-labeled RNA in the isotropic phase was 1.2 Hz.

Bax and co-workers have demonstrated that small changes in bending of the Dickerson dodecamer DNA induced by chemically modified furanose sugars can reliably be detected in partially aligned samples using limited RDC data.[51] Here, we analyzed limited sets of RDC obtained for wild-type as well as 5F-Ura- and 5F-Cyt-substituted HIV-2 TAR RNA (Figure 6). A total of 26 and 28 nucleobase one-bond ^{1}D(H,C) were extracted for partially aligned 5F-Ura- and 5F-Cyt-substituted RNA samples, respectively (Supporting Information Table 1). Unfortunately, the low sensitivity at natural ^{13}C abundance in combination with inadequate water-suppression prevented the reliable quantitation of the RDC data from the ribose moiety. Comparisons with a wild-type RDC data set collected under very similar conditions reveal linear relationships. Linear regression yields a slope of 0.91 with a correlation coefficient of R = 0.92 for 5F-Ura versus wild-type RDCs, a slope of 1.06 with a correlation coefficient of R = 0.89 for 5F-Cyt versus wild-type RDCs, and a slope of 0.85 with a correlation coefficient of R = 0.94 for 5F-Ura versus 5F-Cyt RDCs. The corresponding "best-fit" correlations between all three data sets, wild-type, 5F-Ura, and 5F-Cyt TAR, are shown in Figure 6. We did not attempt to correct for minor differences in effective Pf1 phage concentrations. The good correlations indicate that

(45) Colvin, R. A.; Garcia-Blanco, M. A. *J. Virol.* **1992**, *66*, 930−935.
(46) Jaeger, J. A.; Tinoco, I., Jr. *Biochemistry* **1993**, *32*, 12522−12530.
(47) Bax, A.; Kontaxis, G.; Tjandra, N. *Methods Enzymol.* **2001**, *339*, 127−174.
(48) Prestegard, J. H.; al-Hashimi, H. M.; Tolman, J. R. *Q. Rev. Biophys.* **2000**, *33*, 371−424.
(49) Hansen, M. R.; Hanson, P.; Pardi, A. *Methods Enzymol.* **2000**, *317*, 220−240.
(50) Hansen, M. R.; Mueller, L.; Pardi, A. *Nat. Struct. Biol.* **1998**, *5*, 1065−1074.
(51) Wu, Z.; Maderia, M.; Barchi, J. J., Jr.; Marquez, V. E.; Bax, A. *Proc. Natl. Acad. Sci. U.S.A.* **2005**, *102*, 24−28.

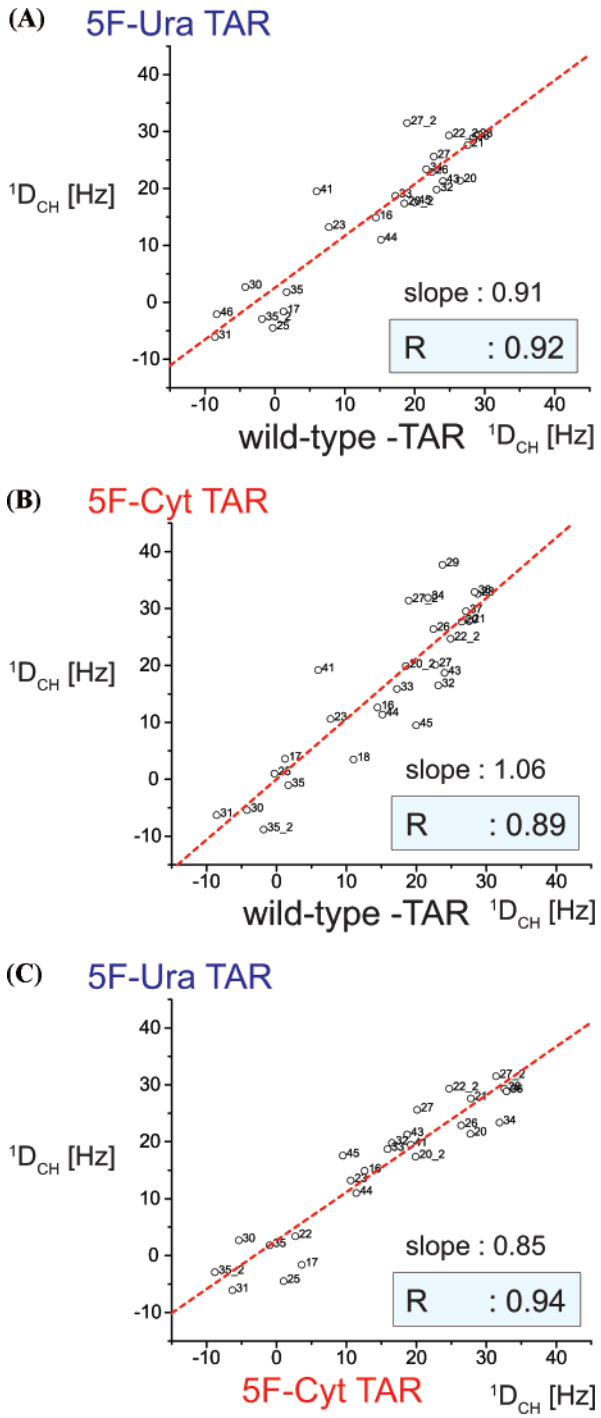

Figure 6. (A) 5F-Ura versus wild-type RDCs, linear regression yields a slope of 0.91 with a correlation coefficient of $R = 0.92$; (B) 5F-Cyt versus wild-type RDCs, slope of 1.06 with a correlation coefficient of $R = 0.89$; and (C) 5F-Ura versus 5F-Cyt RDCs, slope of 0.85 with a correlation coefficient of $R = 0.94$. $^{1}H,^{13}C$-$S^{3}CT^{20}$ experiments[21] were employed to measure residual dipolar one-bond $^{1}H-^{13}C$ coupling constants at natural ^{13}C abundance. 5F-Ura- and 5F-Cyt-labeled RNA samples were partially aligned by the addition of ~25 mg/mL Pf1 phage (ASLA biotech Ltd., Riga, Latvia). The pairwise rmsd for $^{1}J(C,H)$ coupling measurements for 5F-Ura- and 5F-Cyt-labeled RNA in the isotropic phase equals 1.2 Hz. Estimated uncertainties in the anisotropic phase are about 2 times larger on average due to increased line width and slightly lower signal-to-noise ratios.

the uniform introduction of 5F-Ura and 5F-Cyt does not substantially alter the global conformations of 5-fluoropyrimidine-substituted RNA molecules.

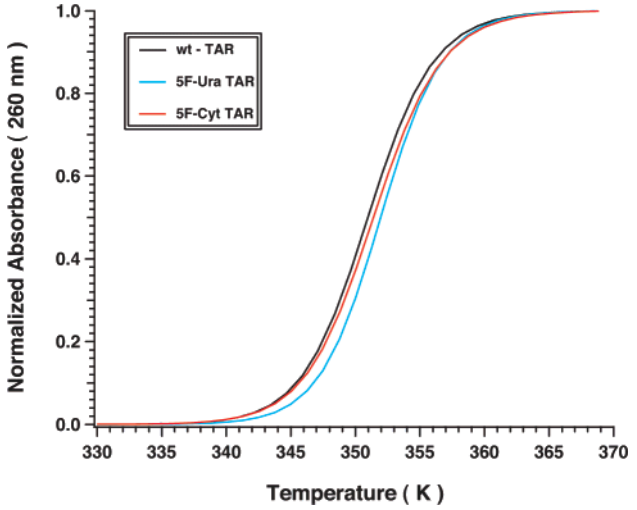

Figure 7. Normalized UV absorbance (260 nm) versus temperature (K) curves for the wild-type (wt-TAR, −) and 5-fluorouridine (5F-Ura TAR, blue −)- and 5-fluorocytidine (5F-Cyt TAR, red −)-substituted HIV-2 TAR RNAs.

Table 2. Thermodynamic Parameters of Wild-type and Fluorinated RNA Constructs

RNA	T_m (K)	$\Delta H_m°$ (kcal mol^{-1})	$\Delta S_m°$ (kcal mol^{-1} K^{-1})
wild-type-TAR	350.48 ± 0.69	−100.48 ± 1.44	−0.29 ± 0.01
5FU-TAR	351.60 ± 0.58	−106.22 ± 1.38	−0.30 ± 0.01
5FC-TAR	351.19 ± 0.54	−99.33 ± 1.59	−0.28 ± 0.01

Thermal Stabilities of Wild-type and 5-Fluoropyrimidine-Substituted HIV-2 TAR RNAs. To determine any thermodynamic effect of 5-fluoropyrimidine substitutions on the stability of the modified RNAs (Figure 1B), thermal melting profiles were recorded for wild-type as well as 5-fluorouridine- and 5-fluorocytidine-substituted HIV-2 TAR RNAs (Figure 7); the resulting thermodynamic parameters are compiled in Table 2. Wild-type HIV-2 TAR RNA exhibited hyperchromicity in a single transition at 350.48 ± 0.69 °C. The thermal melting profiles for 5-fluorouridine- and 5-fluorocytidine-substituted HIV-2 TAR were essentially the same as that measured for wild-type HIV-2 TAR RNA (351.60 ± 0.58 and 351.19 ± 0.54 °C, respectively). The thermodynamic parameters for wild-type, 5-fluorouridine-, and 5-fluorocytidine-substituted TAR RNAs were also quite similar ($\Delta H = -100.48 \pm -1.44$, -106.22 ± 1.38, and -99.33 ± 1.59 kcal mol^{-1}, respectively), clearly demonstrating that the fluorine substitutions do not substantially alter RNA thermodynamic stability.

Discussion

We have established efficient enzymatic syntheses of the fluorinated nucleotide analogues 5F-UTP and 5F-CTP and demonstrated that these can be uniformly incorporated into RNA in template directed transcription reactions using T7 RNA polymerase. The phosphoramidites of 5F-uridine and 5F-cytidine are commercially available for incorporation into synthetic RNAs at defined positions. However, the synthesis of longer RNAs by in vitro transcription can be more cost-effective and provide uniformed labeling of uridine or cytidine residues. Preparation of 5F-UTP and 5F-CTP provides an efficient alternative for ^{19}F-labeling at multiple positions in larger RNAs. Five of the seven enzymes for the synthesis of 5F-UTP are

commercially available, and the remaining three enzymes (*rbs*K, *prs*A, and *ura*P) can be easily prepared from overexpressing bacterial strains. Four of the five enzymes for the synthesis of 5F-CTP can be obtained from commercial vendors, and the remaining enzyme (*udk*) can also be easily prepared from an overexpressing bacterial strain.

A significant number of ^{19}F NMR studies are motivated by the high sensitivity of the fluorine shielding parameters to changes in the local environment. The ^{19}F chemical shift is exquisitely sensitive to changes in the local environment largely due to an anisotropic distribution of electrons in the three 2p orbitals. The van der Waals radius of fluorine is 1.35 Å as compared to 1.2 Å for hydrogen, and apparent RNA structural perturbations upon introducing ^{19}F substitutions into the heterocyclic pyrimidine bases are negligible. It is possible that 5F-pyrimidine substitutions could affect major groove interactions, such as RNA tertiary structure or protein contacts, but these substitutions are readily tolerated in A-form RNA helices. ^{19}F NMR spectroscopy is nondestructive to samples studied, and the introduction of ^{19}F substitutions into the heterocyclic bases of RNA oligonucleotides provides us with uniquely positioned, sensitive reporter groups for many NMR structural studies. The use of ^{19}F NMR spectroscopy as a probe of RNA structure has been extended by investigating the effects of both 5F-Ura or 5F-Cyt substitutions on HIV-2 TAR RNAs.

The assignment of the ^{19}F resonances for 5-fluorocytidine in modified RNA is straightforward and can be achieved using a combination of homonuclear ^{1}H,^{1}H-NOESY and heteronuclear ^{19}F,^{1}H-HOESY experiments. The well-resolved G H1 imino and 5F-C H41/42 amino proton correlations (Figure 2) described in a previous section provide unambiguous anchor points for the sequence-specific assignment of 5-fluorocytidine F5 to H41/42 amino proton HOESY cross-peaks. Additional, weaker correlations to distant H2′ and H3′ ribose protons in HOESY experiments of 5-fluoropyrimidine-substituted RNA are poorly resolved but may help clarify potentially remaining ambiguities (Figure 4). Pioneering work by Horowitz and co-workers demonstrated the utility of homonuclear fluorine experiments. A steady-state NOE measurement with a saturation time of 300 ms identified a sequential pair of 5F-U nucleotides in tRNA.[52] Generally, the straightforward identification of sequential 5-fluoropyrimidines in modified RNAs via the ^{19}F,^{19}F-NOESY (Figure 5) provides invaluable information during the ^{19}F resonance assignment process.

We recently demonstrated that heteronuclear multiple bond correlations (HMBC) applied to 5-fluoropyrimidine-substituted RNA can provide valuable, complementary through-bond connectivities.[4] Vicinal ^{3}J(H6,F)- as well as long-range ^{5}J(H1′,F)-couplings can be exploited for intra-residual magnetization transfer between the ^{19}F nuclei and *J*-coupled protons using a gradient selected HMBC experiment. Unambiguous fluorine chemical shift assignments in 5-fluoropyrimidine-substituted RNA will undoubtedly benefit from an approach combining all NMR experiments described: ^{19}F,^{1}H-HOESY, ^{19}F,^{19}F-NOESY, and ^{1}H,^{19}F-HMBC.[4]

The exchange rate of hydrogens involved in Watson−Crick-type 5F-C−G base-pairs appears to be slower than for normal C−G base-pairs. The terminal G16 imino and the opposing 5F-C46 amino hydrogens can be readily detected at 298 K in 5-fluorocytidine-substituted TAR RNA. Surprisingly, even the unpaired resonances stemming from the apical loop 5F-C30 amino hydrogens give rise to measurable, distinct H41/H42−F5 heteronuclear NOE correlations. The F5 fluorine atom has a negative inductive effect creating a slightly polar (δ^+)-C5−F5-(δ^-) bond. Fluorine substitution at the ortho position enhances the acidity of phenol or aniline ions, with $\Delta pK_a = -1.2$.[53] This inductive effect is likely to be responsible for the change in solvent exchange rate, and it is possible that the C5−F5···H41−N interaction with the exocyclic amino group is responsible for the slower observed C−N bond rotation. The surprising observation of distinct H41/H42−F5 heteronuclear NOE resonances from the apical loop 5F-C30 is consistent with a transiently forming cross-loop base-pair involving the penultimate loop residue G34.[54] This interaction has been proposed on the basis of molecular dynamics simulations,[55] and it was recently suggested that the C30−G34 cross-loop base-pair is required for binding of cyclin T1.[56] While the observed heteronuclear NOEs provide support for the existence of the C30−G34 base-pair, this loop feature is unstable and inherently dynamic in the free form of TAR.

The cytostatic activity of fluoronucleoside and fluoronucleotide metabolites due to mechanisms other than the prevention of DNA synthesis via inhibition of thymidylate synthase is not well understood. The 5′-triphosphate analogues 5F-UTP and 5F-CTP are incorporated into cellular RNA, but no repair processes are known that remove 5-fluoropyrimidines from RNA. Thus, cellular 5-fluorouridine-substituted RNA is thought to account for some aspects of the anticancer activity of 5F-nucleotides by disrupting normal RNA processing and function. This hypothesis gains further support by the fact that 5F-U remains cytotoxic to cells exogenously supplemented with thymidylate synthase.[57] Some studies have suggested that 5F-UTP incorporation into RNA transcripts could disrupt secondary structure formation, thereby providing an explanation for the apparent cytotoxicity.[29,58]

However, we do not observe changes in local structure, global structure, or thermodynamic stability in HIV-TAR that would support this hypothesis. The marginal chemical shift changes observed for exchangeable uridine imino protons in 5-fluorocytidine-substituted and guanine imino protons in 5-fluorouridine-substituted TAR, respectively, indicates near wild-type stacking interactions in modified RNAs. Comparison of the RDCs for substituted and unmodified TAR RNAs indicates that there are no large global structural changes. The melting temperatures of the wild-type TAR RNA and the modified fluorinated analogues differ by less than 2 °C, further corroborating the conclusion of largely unaltered local structural features. Furthermore, titration experiments with argininamide, mimicking the lentiviral Tat protein, reveal no obvious affinity changes for either 5F-Ura- or 5F-Cyt-substituted TAR (data not

(52) Chu, W. C.; Kintanar, A.; Horowitz, J. *J. Mol. Biol.* **1992**, *227*, 1173−1181.
(53) Schlosser, M. *Angew. Chem., Int. Ed.* **1998**, *37*, 1496−1513.
(54) Kulinski, T.; Olejniczak, M.; Huthoff, H.; Bielecki, L.; Pachulska-Wieczorek, K.; Das, A. T.; Berkhout, B.; Adamiak, R. W. *J. Biol. Chem.* **2003**, *278*, 38892−38901.
(55) Nifosi, R.; Reyes, C. M.; Kollman, P. A. *Nucleic Acids Res.* **2000**, *28*, 4944−4955.
(56) Richter, S.; Cao, H.; Rana, T. M. *Biochemistry* **2002**, *41*, 6391−6397.
(57) Spiegelman, S.; Nayak, R.; Sawyer, R.; Stolfi, R.; Martin, D. *Cancer* **1980**, *45*, 1129−1134.
(58) Armstrong, R. D.; Takimoto, C. H.; Cadman, E. C. *J. Biol. Chem.* **1986**, *261*, 21−24.

shown). The nonperturbing nature of the 5F-substitution should permit wide application of this useful specific labeling in RNA structural analysis.

Acknowledgment. We would like to thank Ms. Yelena Pavlova for preparing the *udk* expression construct. M.H. thanks Dr. Bernhard Geierstanger for helpful discussions. This work was supported by the National Institutes of Health (F32 CA80349 to L.G.S., GM-53757 to J.R.W., and GM-66669 to M.H.).

Supporting Information Available: One figure showing imino sequential NOE connectivities for 5-fluorouridine- and 5-fluorocytidine-substituted HIV-2 TAR RNAs. One table with ^1D(H,C) RDC data measured for 5F-Ura- and 5F-Cyt-substituted TAR. This material is available free of charge via the Internet at http://pubs.acs.org.

JA073825I